Validation and Applications of Protein-Ligand Docking Approaches Improved for Metalloligands with Multiple Vacant Sites

Giuseppe Sciortino,[§,#] Eugenio Garribba*[,#] and Jean-Didier Maréchal*[,§]

[§] Departament de Química, Universitat Autònoma de Barcelona, 08193 Cerdanyola del Vallés, Barcelona, Spain

[#] Dipartimento di Chimica e Farmacia, Università di Sassari, Via Vienna 2, I-07100 Sassari, Italy

Corresponding authors. E-mail: garribba@uniss.it (E.G.); jeandidier.marechal@uab.cat (J-D.M.).

Referee1, Referee2, Referee3, Editor

Abstract

Decoding the interaction between coordination compounds and proteins is of fundamental importance in biology, pharmacy and medicine. In this context, protein-*ligand* docking represents a particularly interesting asset to predict how small compounds could interact with biomolecules, but to date very little information is available to adapt these methodologies for metal containing *ligands.* Here, we assessed the predictive capability of a metal compatible parameter set for docking program GOLD for metallo*ligands* with multiple vacant sites and different geometries. The study first presents a benchmark of twenty-five well characterized X-ray metallo*ligand*–protein adducts. In 100% of the cases the docking solutions are superimposable to the X-ray determination and in 92% the value of RMSD between the experimental and calculated structure is lower than 1.5 Å. After the validation step, we applied these methods to five case studies for the prediction of the binding of pharmacological active metal species to proteins: i) the anticancer Cu^{II} complex [Cu^{II}(Br)(2-hydroxy-1-naphthaldehyde benzoyl hydrazine)(indazole)] to human serum albumin (HSA); ii) the active species of antidiabetic vanadium compounds, $V^{IV}O^{2+}$ ion, to carboxypeptidase; iii) the antiarthritic species $[Au^{I}(PEt_3)]^{+}$, to HSA; iv) the antitumor oxalilplatin to ubiquitin (Ub) and, finally, v) the antitumor Ru^{II} compound RAPTA-PentaOH to cathepsin B. The calculations suggested that the binding modes are in good agreement with the partial information retrieved from spectroscopic and spectrometric analysis and allowed us, in certain cases, to propose additional hypotheses. This method is an important update in protein-metallo*ligand* docking which could have a wide field of application, from biology and inorganic biochemistry to medicinal chemistry and pharmacology.

Introduction

The study of the interaction between coordination compounds and proteins is of fundamental importance in biology, pharmacy and medicine.[1] In fact, many metal ions, in a free or complexed form, are part of the active site of proteins and have transport, storage or enzymatic functions. Others metals species are involved in the diagnosis, for example Gd^{III} complexes used for contrast enhancement in magnetic resonance imaging (MRI), or therapy of several diseases, such as the antiulcer agent Bi^{III}-citrate (De Nol™), the antiarthritic triethylphosphine Au^{I} complex (auranofin), the anticancer cisplatin and its derivatives carboplatin and oxaliplatin, the antitumor Ru^{III} compound NAMI-A.[2, 3] Recently, the perspectives of polyoxometalates as potential antitumor, antiviral and antibacterial agents wereas also discussed.[4] For many of these, the interaction with biomolecules is not limited to binding to their therapeutic targets but also to a large number of proteins and peptides that can influence their transport in the blood and cell.

To reach a molecular description of these interactions, different types of experimental techniques are available. X-ray diffraction analysis and NMR can provide an accurate three dimensional description of the protein-metal containing *ligand* (metallo*ligand* [5]) adducts. Other spectroscopic techniques such as EPR, ESEEM, ENDOR, ESI-MS, CD and UV-Vis can give useful information on the protein region where the metal species is bound or on the amino acid residues involved in the coordination, but without reaching a complete 3D description. Our actual knowledge on how metallo*ligands* interact with proteins shows that mainly two binding mechanisms exist: **inert** binding where no direct coordination bonds between the metal and the protein amino acids occur,[6] and **active** or **coordination** binding where one or several coordination bonds are formed (Scheme 1).[7]

Either to predict possible metal mediated binding or enrich partial experimental data, protein-*ligand* docking methods can represent a valuable approach.[8] They have been designed

to generate fast and accurate predictions of the binding of small chemicals with proteins and so determine both relative affinities and binding poses. The background of the docking is thoroughly discussed in refs. 9 and 10, while the historical development of the methods in refs. 11, 12 and 13. Initially the method was applied to the **inert** binding of small organic molecules and only subsequently the first attempts to simulate the interaction of metal containing *ligands* were made (Scheme 1, a).[14, 15] However, like for most force field based approaches, dealing with metallo*ligands* is far from straightforward because the effect of the metal and the possibility that one or more coordination bonds are formed must be considered. Even if covalent docking methods are available for software such as GOLD,[16] Autodock,[17] CovalentDock,[18] and Docktite,[19] their application to metal complexes have several limitations: for example, the formation of the chemical bonds is forced *a priori* through energetic restraints and is generally limited to specific bond classes ~~distances and angles~~.

To overcome these limitations, we recently started a series of explorative works for updating protein-*ligand* docking methods. Since many metal mediated protein-*ligand* interactions are **active** in nature, we generated a new series of parameters in the GOLD program to treat the **coordination** binding (Scheme 1, b and c). To do so, we took advantage of the ~~polarity terms provided by general~~ hydrogen bond terms ~~in docking~~ implemented in docking scoring function ~~programs parameters~~ to include bond parameters in the program. The work allowed to reproduce with good agreement the X-ray structures of thirty-nine proteins-metallo*ligands* with the monodentate binding of only one amino acid residue to the metal (Mg, V, Cr, Mn, Cu, Fe, Co, Ni, Cu, Zn, Ru, Rh, Re, Os, Pt, and Au).[20, 21] However, in this pioneering study, we only considered the possibility that the metal could interact throughout a unique well defined and oriented vacant site of the metal; in this case, the stereochemistry and chirality could not change (Scheme 1, b). More general problems like metal species with multiple accessible sites, possibility of formation of various isomers and

other electronic based geometrical constraints have not been considered because of the substantial shift in complexity it represents.

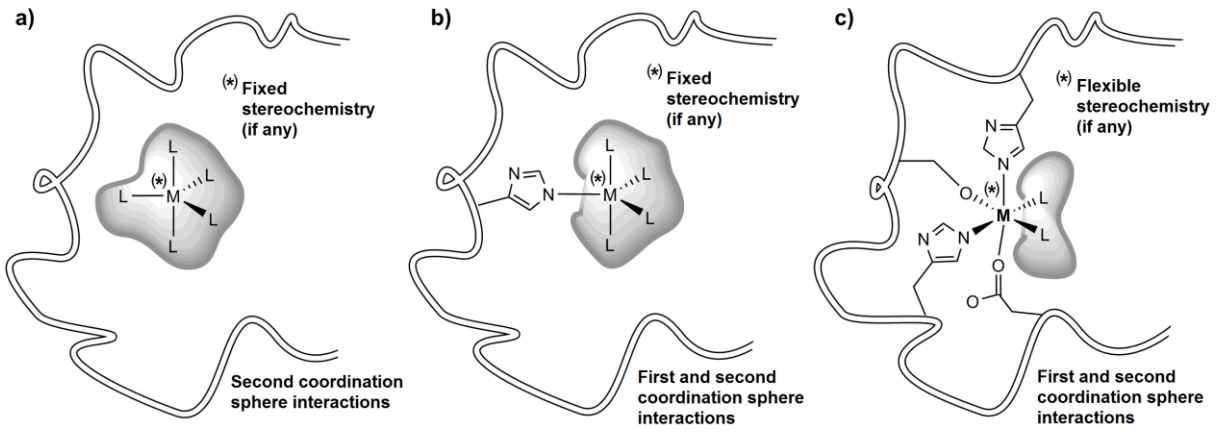

Scheme 1. Metallo*ligand*–protein docking: a) **inert** binding with only second coordination sphere interaction, fixed stereochemistry and chirality; b) **active** binding with one coordination bond, fixed stereochemistry and chirality and c) **active** binding with several coordination bonds, stereochemistry and chirality defined by these interactions (this work).

Here, we report how our novel metal compatible docking strategy provides a generalized framework for the prediction of the interaction of metallo*ligands* with proteins for any ~~multiple~~number of vacant sites (Scheme 1, c). Twenty-five structures formed by main group and transition metal containing *ligands* with coordination numbers 4, 5 and 6, ~~with~~ square planar, tetrahedral, trigonal bipyramidal, square pyramidal and octahedral geometry, and 2, 3 or 4 coordination vacancies ~~bonds~~ were examined. After a first validation step, the study was further expanded to test the potentiality of the method for the prediction on metal-protein systems for which no X-ray structures are reported and only few spectroscopic data were available: i) the anticancer Cu^{II} complex [Cu^{II}(Br)(2-hydroxy-1-naphthaldehyde benzoyl

hydrazine)(indazole)] with human serum albumin (HSA);[22] ii) the active species generated under the physiological conditions of antidiabetic vanadium compounds, $V^{IV}O^{2+}$ ion, with carboxypeptidase;[23, 24] iii) the antiarthritic species $[Au^{I}(PEt_3)]^{+}$, formed in aqueous solution by the anti-arthritic compound auranofin, with HSA;[3a, 25] iv) the antitumor compound oxalilplatin, $[Pt^{II}$(dach)(oxalate)], where dach is diaminocyclohexane, with ubiquitin (Ub);[3c, 26, 10b] and v) the antitumor Ru^{II} compound RAPTA-PentaOH (RAPTA = Ru(II)-arene-1,3,5-triaza-7-phosphatricyclo-[3.3.1.1] decane) with cathepsin B.[3c] The interested readers in the chemistry and biochemistry of the five elements studied are referred to some excellent books.[27]

The results show that the general scheme expand the framework of protein-*ligand* docking so to become valid predictive for the most of metallo*ligand*–protein interactions, and that this approach could have a general applicability not only in medicinal chemistry and pharmacology but also in the entire field of bioinorganic chemistry and biology.

Computational Section

Protein and Metallo*ligand* Setup. For the ~~first part of the study on the~~ validation of the method, all the X-ray metallo*ligand*-protein structures (Table S1 of Supporting Information) were cleaned and prepared for the docking removing the crystallographic small molecules and, subsequently, the metallo*ligands* (i.e., the metal ions with their first coordination sphere organic ligands) were removed from the protein binding site and the relative coordinates saved in a new .mol2 file. For the ~~second part of the study on the~~ application of the method to systems for which the X-ray determination of the metallo*ligand*-protein adducts is not available, the structure of the protein was taken from the Protein Data Bank (PDB),[28] while

that of the metallo*ligand* was obtained from the Cambridge Structural Database (CSD),[29] PDB, or optimized by Density Functional Theory (DFT) methods.

Before the docking simulations, the hydrogen atoms ~~and the titratable protons~~ were added to the protein through the algorithm implemented in UCSF Chimera Software,[30] and the metal atoms were pre-treated adding dummy hydrogens on the free coordination positions liable to interact with the protein donors.[21]

Docking Protocol. Docking calculations were performed with the software GOLD 5.2[16a] using GoldScore function.[31] The parameters optimized in our previous study[21] were further tuned on the new dataset of twenty-five metal complexes analyzing the docking poses in terms of binding site of the best pose, spatial orientation, RMSD value and bond lengths, until reaching the best solution located in the correct binding site for all the structures of the same metal. The only change needed was the increasing in the value for S(Met) (SACC in Table S5 of Supporting Information) that was brought from -15 to -30.

The metal complexes, separated from the protein, were preliminary treated by virtually activating the vacant coordination sites through a dummy hydrogen atom according to the procedure recently established.[20-21, 32] To prevent any bias, their coordinates (with both rotational and translational transformations) were randomized and subsequently blindly re-docked to the protein without any geometrical constraints or energy restraints. ~~Briefly~~, To account for the formation of coordination bonds, the docking update consists in the description of these interactions with the hydrogen bond function implemented in GoldScore. The software recognizes the metal as a *hbond* donor liable to interact with the *hbond* acceptors of protein. In other words, thinking in terms of Lewis acid and base theory, the acid acceptor results translated from the metal to a fictitious proton located at the metal vacant bond axis to preserve the coordination directionality.[20-21]

Genetic algorithm (GA) parameters were set at 50 runs and minimum of 100,000 operations. All the other parameters – pressure, number of islands, niche size, crossover, mutation and migration – were set to default.

In the validation part, the dockings were carried out considering flexible all the ligands through the application of the GOLD algorithm, while the protein residues were considered rigid as in the X-ray structure because the amino acid side chains are already in the ideal conformation to bind the metal; this is considered enough for the validation stage. In the application part, in which the predictive capability of the method was assessed, the flexibility of the residue side-chains in the region of interaction (approximately the residues within 5 Å radius from the center of the region) was taken into account using the rotamer libraries[33] implemented in GOLD software.

Blind docking simulations were performed considering an evaluation sphere with a radius of 20 Å centered on the selected binding site. The solutions were analyzed by means of GaudiView, an *in house* interface freely accessible from InSiliChem webpage.[34]

The docking solutions were assessed through several criteria: i) the mean (F_{mean}) and the highest value (F_{max}) of scoring *Fitness* of GoldScore reported in eq. 1 associated with each pose; ii) the population of the cluster containing the best pose; iii) the root mean square deviation (RMSD) of the poses calculated on the heavy atom as reported in eq. S1 of Supporting Information; iv) the absolute percent deviation (APD) and the mean absolute percent deviation (MAPD) of the metal–D^{aa} bond length, where D^{aa} indicates the amino acid donor of protein, reported in eqs. S2 and S3 and v) the position in the *Fitness* ranking of the computed cluster.

The scoring *Fitness* of GoldScore is:

$$Fitness\ (F) = \alpha \cdot S_{hbond}^{ext} + \beta \cdot S_{vdW}^{ext} + \gamma \cdot S_{hbond}^{int} + \delta \cdot \left(S_{vdW}^{int} - S_{tors}\right) \quad (1)$$

where S_{hbond}^{ext} and S_{vdW}^{ext} describe the hydrogen (*hbond*) and van der Waals (*vdW*) intermolecular interactions, S_{hbond}^{int} and S_{vdW}^{int} the corresponding intramolecular interactions, S_{tors} the energy change related to the molecular torsions, and α, β, γ, and δ are empirical parameters defined by default in GOLD software.

Results and Discussion

Dataset. A benchmark dataset of twenty-five high quality X-ray structures, in which a protein is bound to a metallo*ligands* through amino acid donors (D^{aa}) with at least two and up to four coordination bonds, was collected. All the structures (shown in Figure 1 and listed in Table S1 of Supporting Information) were taken from PDB.[35a-c, 35f-h, 35j-u] The dataset was built as large and diversified as possible considering all the high quality structures reported in the PDB of metal species bound to a protein with multiple coordination bonds. The dataset includes a wide range of biologically relevant metals (Mg, Mn, Fe, Cu, Zn, Ru, Pt), donor types (N_{His}, S_{Met}, S^{-}_{Cys}, O^{-}_{Tyr}, O^{-}_{Ser}, $COO^{-}_{Asp/Glu}$, and $N_{Lys/amine}$), coordination numbers and geometries. The dataset is summarized in Table 1.

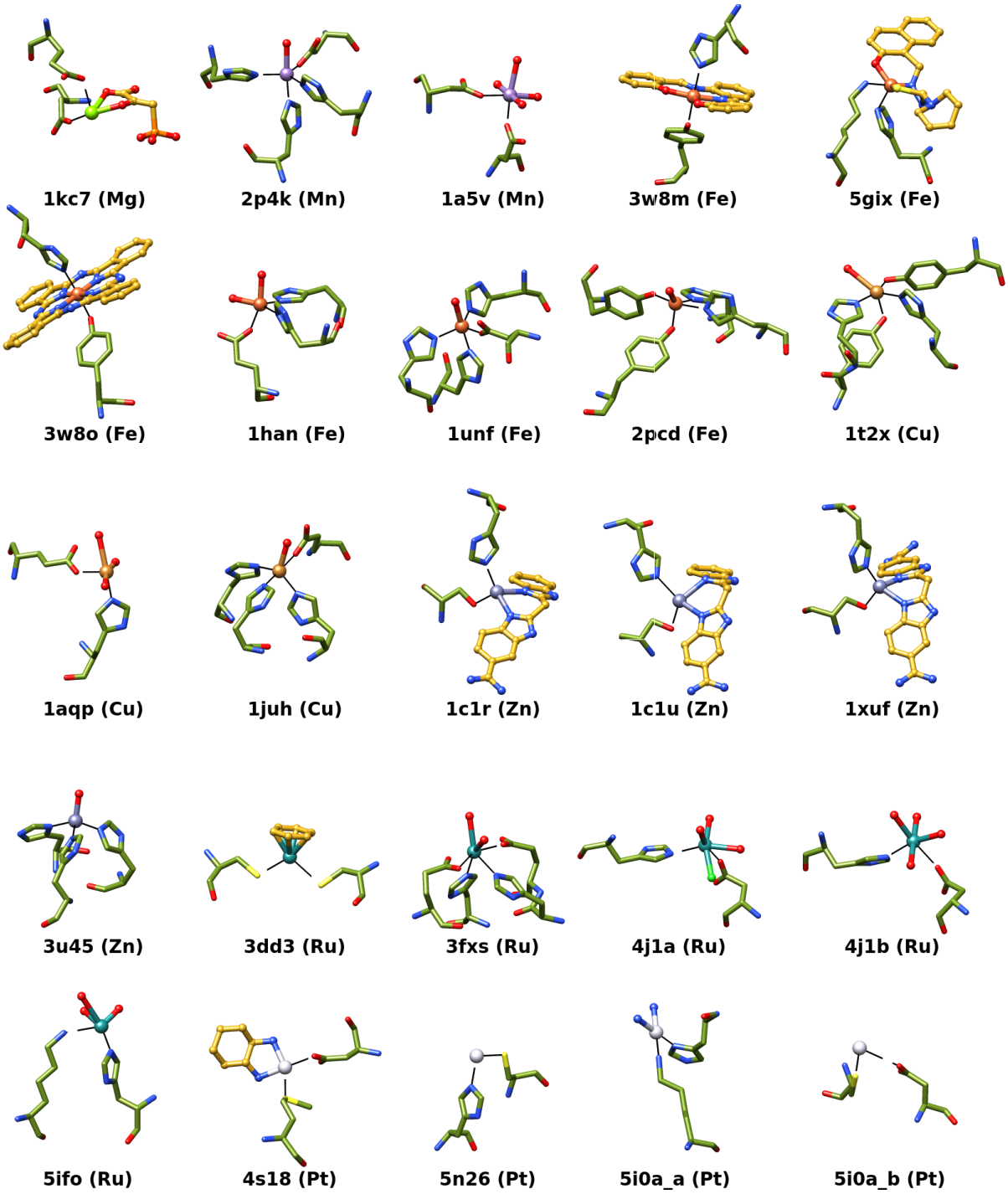

Figure 1. Graphical representation of the dataset. The region of the protein, where the interaction with the metal complexes occurs, ~~areis~~ represented. The ligands, the metals and amino acid residues are shown with different colors. Below each structure, the PDB code and the metal (in parentheses) are indicated.

Table 1. Metals and geometry distribution in the dataset.[a,b]

	Geometry (number of amino acid donors)					
Metal	td (n° D^{aa})	sp (n° D^{aa})	tbp (n° D^{aa})	spy (n° D^{aa})	oct (n° D^{aa})	Total
Mg					1(4)	1
Mn			1(4)		1(2)	2
Fe			2(4)	1(2)	2(2), 1(4)	6
Cu			1(4)	1(4)	1(2)	3
Zn	3(2), 1(3)					4
Ru	1(2)				3(3), 1(4)	5
Pt		4(2)				4
Total	5	4	4	2	10	25

[a] Geometry: td = tetrahedral; sp = square planar; tbp = trigonal bipyramidal; spy = square pyramidal; oct = octahedral. [b] D^{aa} stays for amino acid donor.

Validation. The new parameters for metal–proteins interactions, recently discussed[21], were applied to twenty-five systems with multiple coordination bonds (from two to four, see Table 1), which were blindly redocked with the objective to reproduce the X-ray crystallographic structures.

The data show that the success percentage was 100% considering that, in all the cases, the solution suggested by docking is superimposable to the experimental structure and the metal environment is the same (both as coordination mode and orientation with respect to protein) as the X-ray determination. The comparison between the calculated docking poses (in blue) and the X-ray data (in orange) is reported in Figure 2.

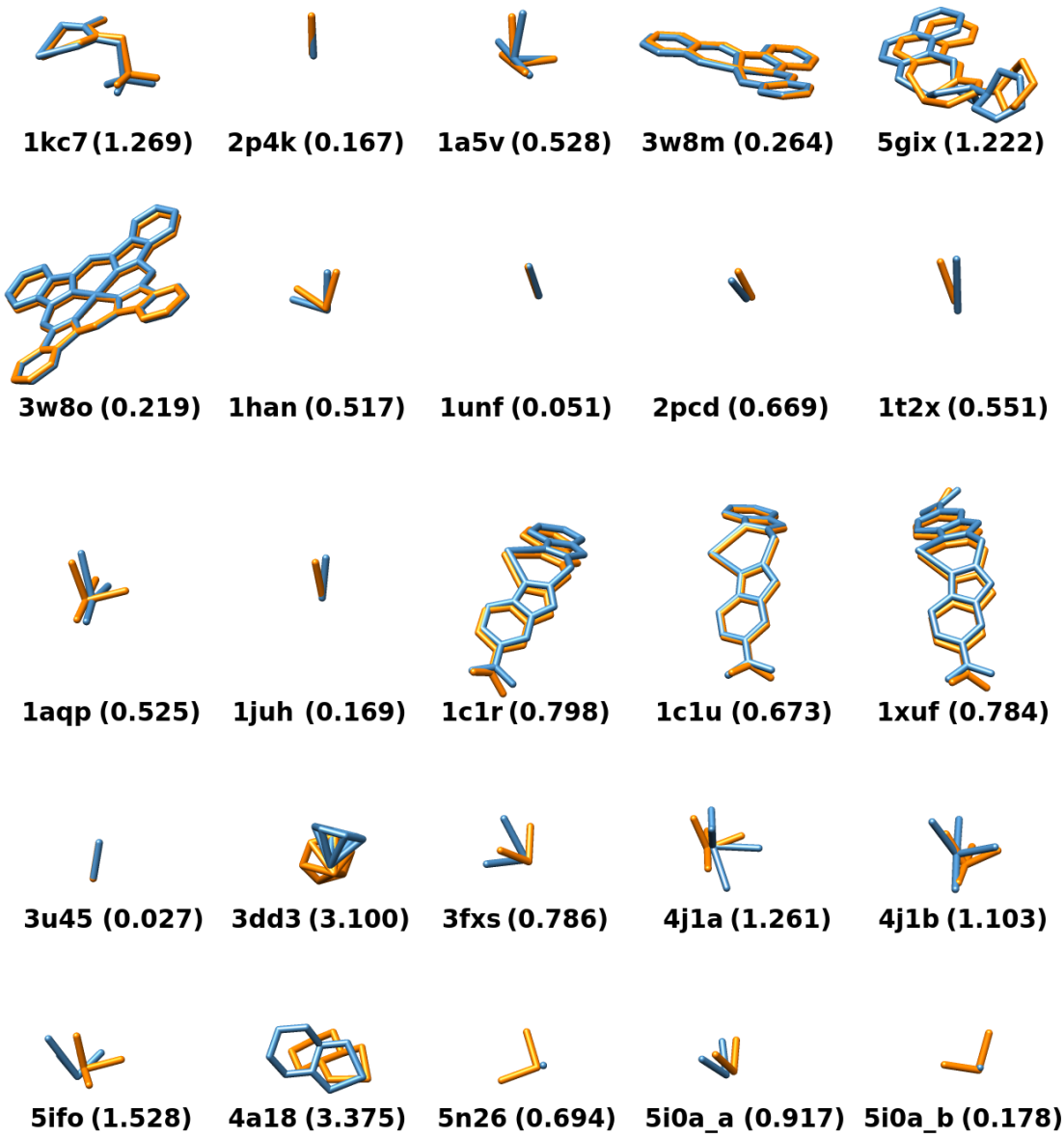

Figure 2. Overlap of the best docking pose (in blue) and the X-ray structure (in orange) of the twenty-five metal structures of the dataset. For each structure, the PDB code and the RMSD value (in parentheses) for each solution are reported.

The RMSD for each docked pose and MAPD for selected structural parameters are reported in Table 2. The value of 0.855 Å obtained for the mean RMSD is very small and confirms the high capability of prediction of the method, both in terms of binding site recognition and donors discrimination. Analogous considerations are valid for the MAPD relative to the bond

lengths (6.95%) and demonstrate the high accuracy of this approach in the prediction of the overall geometry of the binding sites. The standard deviations correspond to an error distribution very close to the mean value of the set, allowing us to conclude that the method is highly efficient. Moreover, for 92% of the structures considered (twenty-three out of twenty-five), the RMSD between the experimental and the calculated structure is lower than 1.5 . An in-depth examination of the GoldScore values and overall population of the predicted sites shows that the best docking poses have the highest fitness in the 88% and are found in the most populated cluster in the 92% of the cases (Figure 2 and Table S1 of Supporting Information).

Table 2. Values of the mean RMSD and MAPD for the bond lengths obtained for the dataset of twenty-five metallo*ligand*–protein structures.

Dataset of twenty-five metallo*ligand*–protein structures		
	Mean RMSD [a,b]	MAPD (bond lengths)
	0.855	6.95%
SD [c]	0.827	7.00%

[a] Value reported in Å. [b] RMSD computed with software UCSF Chimera. [c] Standard deviation (SD).

The results discussed above demonstrate that the method is generalizable, in principle, to any metallo*ligand*–protein system, independently of the number of donors bound to the metal. To investigate its possible applications to in the real world, several case studies – for which no X-ray structures are available – were investigated. We selected systems involving the interaction of the Cu^{II}, $V^{IV}O$, Au^{I}, Pt^{II} and Ru^{II} species with important pharmacological and

biological targets, for which only spectroscopic or spectrometric evidence of the binding interaction is reported in the literature).

Case Studies. (1) Interaction of Anticancer Cu^{II} species with Human Serum Albumin. The research on copper coordination compounds as antiproliferative agents has drastically increased in the last few years as demonstrated by the high number of publications in the period 2008-2018.[36] ~~In this context, h~~ In this context, human serum albumin (HSA) is considered a potential drug delivery system because it is a non-toxic, non-antigenic, biocompatible and biodegradable endogenous protein, and it is able to interact with Cu species.[37] ~~uman serum albumin (HSA) is considered a potential drug delivery system because it is a non-toxic, non-antigenic, biocompatible and biodegradable endogenous protein, and it is able to interact with Cu species.~~

To prove the predictiveness of our metal compatible docking methodology, we blindly docked the Cu^{II} anticancer complex [Cu(Br)(L)(indazole)] (HL = 2-hydroxy-1-naphthaldehyde benzoyl hydrazine) to subdomain IIA of HSA, based on a recent study showing the interaction of the drug with this domain.[22]

The docking calculations were carried out using a deposited crystallographic coordinates of an unbound HSA (PDB: 1bj5 [38]) and the X-ray structure of [Cu(Br)(L)(Indazole)], deposited in the CSD (CSD code: 1046819 [22]). Side chain flexibility was introduced in the interaction region using the rotamer libraries implemented in GOLD[33] for Lys199, His242 and nearby Lys190 residues. The two lysine residues were considered in their neutral form to be able to bind the metal with the free electron pair.

The results show that in the best docking solution (F_{max} = 69.04) two coordination bonds between Cu and the residues of Lys199 and His242 of the IIA hydrophobic subdomain of HSA are formed (Figure 3 and Table S2 of Supporting Information). The calculated geometry

is an intermediate between the trigonal bipyramid (with the two O donors in the axial position) and square pyramid (with N(His242) in the apical site) and the predicted bond lengths are 2.327 Å for Cu–NH_2(Lys199) and 2.262 Å for Cu–N(His242), in line with the values reported in literature for the interactions Cu^{II}–N_{amine} and Cu^{II}–$N_{imidazole}$.[39] Overall, the results agree well with the experimental electron density map and X-ray structure of the adduct CuL–HSA (not yet deposited),[22] and suggest that the monodentate weak ligands Br^- and indazole undergo dissociation in the presence of the protein and are replaced by two residues of albumin.

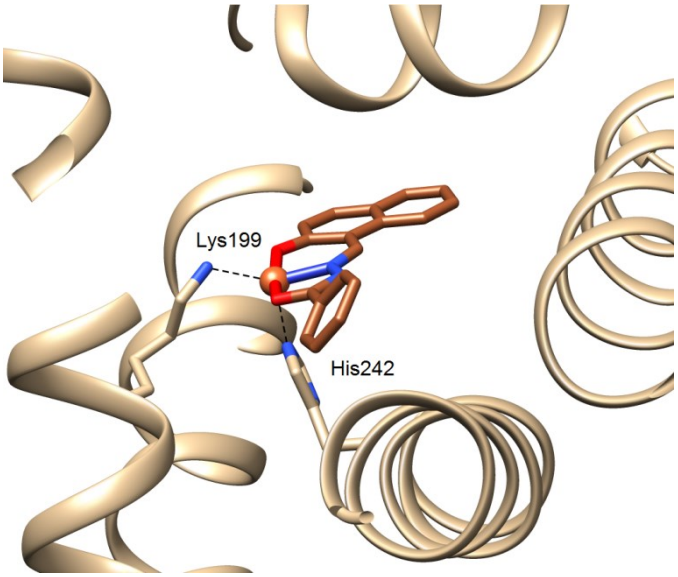

Figure 3. The binding site proposed by docking calculations for the interaction of [Cu(Br)(L)(indazole)] with the IIA domain of HSA. The adduct is formed after the replacement of Br^- and indazole ligands by Lys199 and His242 donors.

Taking into account the good result obtained for this case study, for which the structure has been determined through the X-ray analysis, we continued the study with (metal complexes)–protein adducts for which none crystallographic information are available at all.

Case Studies. (2) Binding of $V^{IV}O^{2+}$ Ion to Carboxypeptidase. The two most interesting pharmacological applications of $V^{IV}O$ compounds are as antidiabetic agents for the treatment of type II diabetes,[40] and as potential antitumor drugs.[40g, 41] Vanadium forms also polyoxovanadates recently proposed as potential antitumor, antiviral and antibacterial agents.[4] In the blood serum, orally administered V compounds, undergo speciation to form $(V^{IV}O)$(hTf) and $(V^{IV}O)_2$(hTf) and $H_2V^{V}O_4^-$, which should cross the cell membrane via endocytosis or through the anion channels.[42] In the cells V^{V} is reduced to $V^{IV}O^{2+}$ [43] and, therefore, this ion could be one of the active species in the organism.[40f, 40h, 44] Therefore, the interaction of V with proteins is fundamental to understand its antidiabetic and antitumor action. In the early 1970s, Chasteen and co-workers employed Electron Paramagnetic Resonance (EPR) patterns of $V^{IV}O^{2+}$ to extract specific information on the $V^{IV}O^{2+}$ binding in various peptides and proteins,[45] but up to now no X-ray determination has been reached for this particular system.

In this study, we used docking methods to revisit the data reported for the interaction of $V^{IV}O^{2+}$ with carboxypeptidase,[23, 24] an enzyme that hydrolyzes the peptide bond at the *C*-terminal end of a protein [46], which represents in this study a model protein. The prediction of the binding site was carried out on the X-ray structure deposited in PDB for carboxypeptidase (1cpx [47]). The geometry of $[V^{IV}O(H_2O)_4]^{2+}$ ion was DFT optimized then the four equatorial water molecules were removed and the coordination positions were activated for protein binding as described in the Computational Section. After determining the experimental-suggested interaction region,[23,24] the flexibility of the side chains which could bind $V^{IV}O^{2+}$ was considered applying the GOLD rotamer libraries.[33]

The results for the interaction between $V^{IV}O^{2+}$ and carboxypeptidase (Table S3 of Supporting Information), show a unique cluster of 50 docking poses with the highest scoring

(F_{max}) of 54.31 GoldScore *Fitness* units. The best predicted solution indicates $V^{IV}O^{2+}$ binding with three different donors, two histidines (His69 and His196) and one glutamate residue (Glu72). This site is identical as that of Zn-carboxypeptidase,[48] and this is in agreement with the similar chemical behavior of Zn^{2+} and $V^{IV}O^{2+}$ ions.

The geometry for the adduct $V^{IV}O^{2+}$–carboxypeptidase is a square pyramid with a vacant coordination position, reasonably occupied by a water molecule in the real system. The predicted bond lengths are 2.322 Å for V–N(His196), 2.295 Å for V–N(His69) and 2.259 Å for V–COO^-(Glu72), comparable with the experimental values for V^{IV}–N(imidazole) coordination[49] and V^{IV}–COO^-(acetate) distances.[50] The angles O=V–D^{aa} range from 101.4 to 106.1°, indicating the vanadium is slightly above the plane spanned by the four equatorial donors. The best solution is shown in Figure 4 and is in agreement with that hypothesized before by DeKoch *et al*. on the basis of EPR data,[23] and then by Sanna *et al*. after the comparison between the experimental and DFT calculated ^{51}V hyperfine coupling constant A_z [24] (A_z is 175.8 × 10^{-4} cm^{-1} below pH 5 and 165.9 × 10^{-4} cm^{-1} above pH 5 [23]). This means that at acidic pH values – with the imidazole nitrogen of His protonated – only the carboxylate group of Glu72 is able to bind V accounting for the high value of A_z, while around the neutrality – with the deprotonation of histidines – the side chains of His69 and His196 add to Glu72.

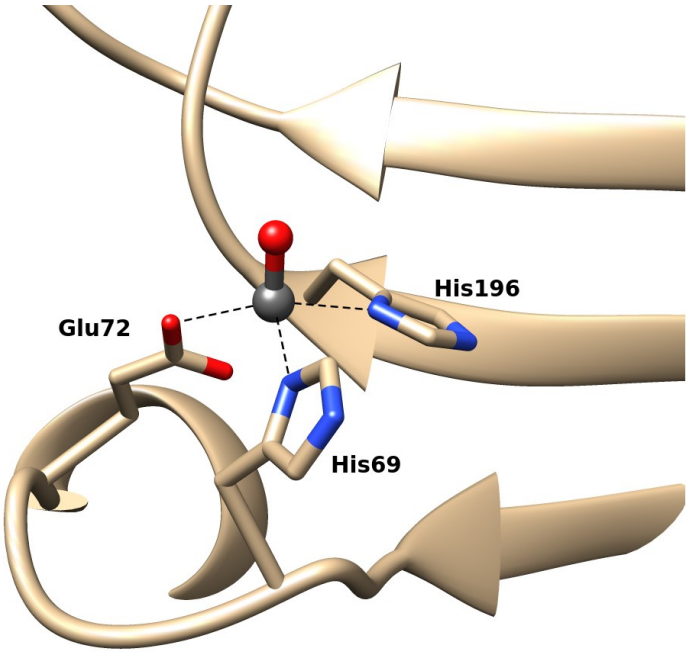

Figure 4. The binding site proposed by docking calculations for the interaction of $[V^{IV}O(H_2O)_4]^{2+}$ to carboxypeptidase. The adduct is formed after the replacement of three H_2O molecules by His69, Glu72 and His196 donors.

Case Studies. (3) Binding of $[Au^{I}(PEt_3)]^{+}$ to Human Serum Albumin. From many years gold complexes have been studied for their pharmacological action and potential medicinal applications.[51] In 1985, an orally active gold drug named auranofin ((2,3,4,6-tetra-O-acetyl-1-thio-β-D-glucopyranosato-*S*)(triethylpho-sphine)gold(I)) was introduced for the treatment of rheumatoid arthritis.[3b, 3c, 25] Auranofin was shown to be also highly cytotoxic to tumor cells in culture and is currently being evaluated for the treatment of chronic lymphocytic leukemia (CLL) in phase II clinical trials.[52, 53] Other Au^{I} species based on the same $[Au^{I}(PEt_3)]^{+}$ moiety – i.e. $Et_3PAu^{I}Cl$, $Et_3PAu^{I}CH_3$, $Et_3PAu^{I}CN$, $Et_3PAu^{I}SCH_3$, $Et_3PAu^{I}SCN$, $Et_3PAu^{I}SPh$ –were evaluated for *in vitro* cytotoxicity against both B16 melanoma cells and P388 leukemia cells and *in vivo* antitumor activity against P388 leukemia in mice.[54] Serum albumin appears to be

the protein candidate to transport Au^{I} species in human organism. However, no X-ray structure of the adduct $Au^{I}(PEt_3)$–HSA is yet available.

In this study, the binding site of HSA for the $[Au^{I}(PEt_3)]^{+}$ moiety, formed upon the release of the anionic ligand by auranofin and its derivatives, was studied. The docking calculations were carried on the two folding states of the protein in the presence (PDB: 1bj5 [38]) or absence (PDB: 1ao6 [55]) of fatty acids. The geometry of $[Au^{I}(PEt_3)]^{+}$ was taken from the structure deposited in the PDB (code 1e3b [56]). The calculations were performed exploring the HSA domain I containing the Cys34 residue. The side chain flexibility in solution was taken into account applying the Gold rotamer libraries[33] for Cys34 and the neighboring residues ~~of~~ Asp38 and Tyr84. The results indicate, for both the folding states, a significant preference of $[Au^{I}(PEt_3)]^{+}$ for Cys34, the highest affinity of 41.76 GoldScore *Fitness* units (F_{max}) being found for fatted HSA. This appears to be in agreement with the previous experimental evidence. For example, Sadler and coworkers studied the reaction of auranofin with HSA by ^{1}H NMR and concluded that the drug reacted with Cys34,[57] this finding being confirmed by Shaw and coworkers, who proposed that binding of the $Au^{I}(PEt_3)^{+}$ fragment of the gold drug to Cys34 for bovine serum albumin (BSA).[58] Furthermore, Dean *et al*. showed very recently that the fragment $[Au^{I}(PEt_3)]^{+}$ was transferred to recombinant human serum albumin (rHSA) and that PEt_3 promoted significant modification of Cys34.[53]

Rather interestingly, the docking analysis suggests the possible formation of adducts $Au^{I}(PEt_3)^{+}$–His; in particular, a secondary binding site (F_{max} = 31.4) could be represented by His146, located in the hydrophobic region of the protein. This is an important insight provided by docking and it is in line with the hypothesis of Sadler and co-workers, who found that the model protein cyclophilin binds $[Au^{I}(PEt_3)]^{+}$ not with one of the four Cys of its structure but with His133.[56]

The two proposed binding sites are shown in Figure 5. The calculated structures exhibit a linear coordination geometry with the bond lengths Au–S(Cys34) and Au–N(His146) of 2.391 and 2.111 Å, respectively, in agreement with those determined by EXAFS (2.27 and 2.06 Å [59]). The P–Au–S/N angles are 175.7 and 167.2 Å.

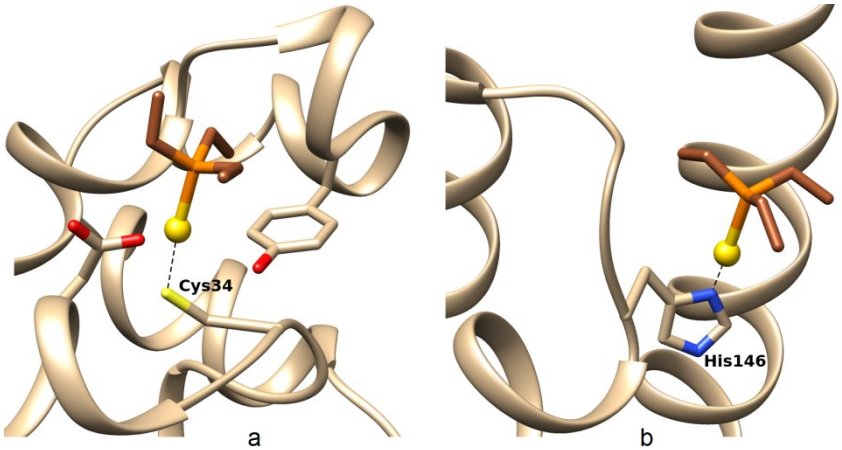

Figure 5. The two binding sites proposed by docking calculations for the interaction of $[Au^{I}(PEt_3)]^{+}$ moiety to HSA: a) primary binding site with coordination of Cys34 and b) secondary binding site with Au^{I} coordinated to His146.

Case Studies. (4) Binding of Oxalilplatin to Ubiquitine. The discovery of cisplatin, *cis*-$[Pt(NH_3)_2Cl_2]$, has been a watershed in the medicinal inorganic chemistry.[60] However, due to its negative secondary effects, over the last decades the research has been focused on alternative anticancer platinum compounds to replace the first generation drug.[3a, 3c, 61] The second generation of platinum antitumor compounds, including carboplatin and oxalilplatin among others, have shown lower toxicity avoiding several side effects.[62] In particular oxaliplatin, [Pt(dach)(ox)] with dach = 1*R*,2*R*-diaminocyclohexane and ox = oxalate, was introduced for clinical use in Europe Union since 1999 and in 2002 in United States, is much

less nephro- and ototoxic than cisplatin and represents an alternative in the case of cisplatin-resistant tumors.[26, 10b, 3c, 63] From a chemical point of view the [Pt(dach)(ox)] complex under physiological conditions, after releasing the labile oxalate ligand, forms the $[Pt^{II}(dach)]^{2+}$ moiety with two vacant coordination positions liable to interact with serum low- and high-molecular mass bioligands such a proteins.

In this work we focus on the interaction of oxalilplatin with ubiquitin (Ub), largely studied as a model for serum proteins because it is a relative small polypeptide (8.6 kDa) containing 76 amino acids and a limited number of potential coordinating residues. In several recent papers, the formation of mono-adducts [Pt(dach)]–Ub was proved using high-resolution electrospray ionization mass spectrometry (ESI-MS) and diverse tandem mass spectrometric (MS/MS) techniques and the monodentate coordination of Met1 and His68 residues was proposed as the preferential binding mode of oxaliplatin.[64] No bidentate coordination of ubiquitin to the two free site of the moiety $[Pt^{II}(dach)]^{2+}$ was individuated and, for this reason, an unambiguous characterization of the system – in particular, the 3D representation of the interaction – remains to be reached. Obviously docking could help to throw light on this topic.

The docking analysis was performed using the X-ray structure of the bovine ubiquitin (PDB: 3h1u [26]) while the Cartesian coordinates of $[Pt^{II}(dach)]^{2+}$ were extracted from ref. [35j] (PDB code: 4s18). The calculations were carried out exploring the proteic space containing the potential coordinating side chains, among them Met1, Glu64, and His68. The side chain flexibility in solution was taken into account applying the Gold rotamer libraries[33] for Met1, Glu64 and His68, and their neighboring residues. The results suggest the formation of three different [Pt(dach)]-Ub adducts: i) the binding of S(Met1) at the *N*-terminal site with fourth Pt coordination site reasonably occupied by a hydroxyl or a water ligand (F_{max} = 45.65; population = 50/50); ii) the simultaneous binding of N(His68) and N(Lys6) (F_{max} = 50.76; population = 49/50) and iii) the bidentate coordination of ubiquitin through the COO(Glu16)

and COO(Glu18) donors (F_{max} = 48.46; population = 49/50). All the three solutions reach comparable scoring values and fall in a fully populated cluster in the first ranking position of the respective docking assay (Table S4 of Supporting Information).

The first two found binding sites (Figure 6, a and b) appear to be in agreement with the previous experimental evidences, even if an important comment must be made: while mass spectrometric methods are not able to discriminate between the mono- and bidentate coordination of Ub, docking indicates that the binding of Met1 is not assisted by other residues; in contrast, the interaction with Lys6 – which was not considered until now in the literature – can stabilize the binding of His68. The calculated structures exhibit a square planar geometry with the bond lengths Pt–S(Met1), Pt–N(His68) and Pt–N(Lys6) of 2.034, 2.256 and 2.456 Å, respectively.

The third binding site involves the coordination of COO(Glu16) and COO(Glu18) to $[Pt^{II}(dach)]^{2+}$ moiety and can be predicted on the basis of this study; it is strongly stabilized by a network of hydrogen bond between carboxylate groups of Glu18 and Asp21 and carbonyl of Glu16 to NH_2 groups of dach ligand (Figure 6, c). The distances Pt–O(Glu16) and Pt–O(Glu18) are 2.240 and 2.364 Å.

Finally, docking simulations suggest that no interaction with Glu64 exists, confirming the previous published data.[64]

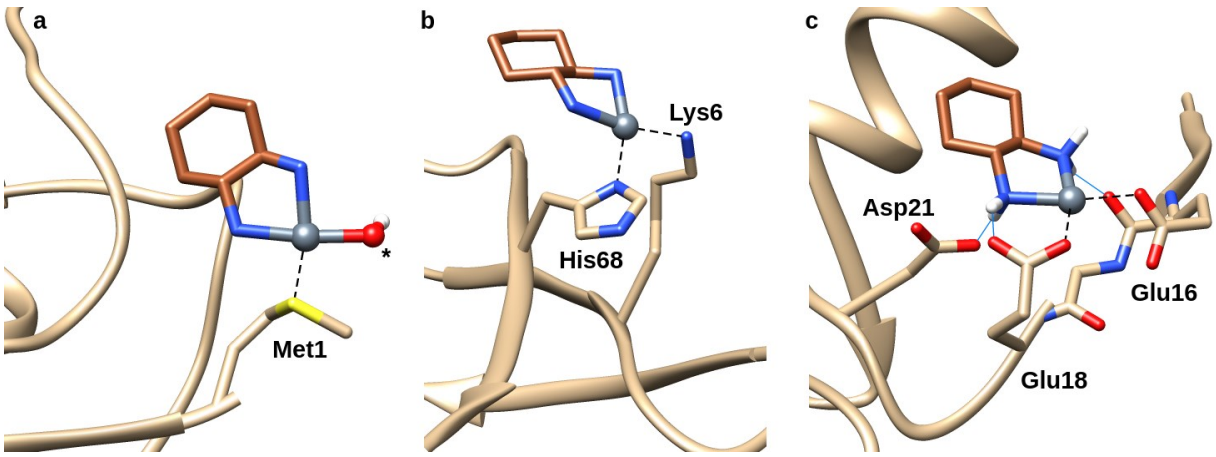

Figure 6. The three binding sites proposed by docking calculations for the interaction of oxalilplatitin with ubiquitin: a) binding site with the coordination of Met1 and the fourth Pt site occupied by a hydroxyl or a water ligand (with the asterisk); b) binding site with the coordination of Lys6 and His68 and c) binding site with the coordination of Glu16 and Glu18. The hydrogen bonds are also highlighted with the full line.

Case Studies. (5) Binding of Ru RAPTA-PentaOH to Cathepsin B. As a final illustrative case for the predictiveness of our docking update for transition metal, we focused on ruthenium drugs. A large number of ruthenium compounds have been synthesized and tested for their anticancer properties.[65] Two of them based on Ru^{III}, named NAMI-A and KP1019, are now under clinical trials.[66, 67] So far, the experimental evidence has shown that those Ru^{III} species could be reduced by bioligands of the organism to Ru^{II}, which explicate the pharmacological activity.[68, 69] On the basis of this finding, the anticancer activity of a series of Ru^{II} compounds has been examined and, among them, $[Ru^{II}Cl_2(\eta^6\text{-arene})(pta)]$, where pta is 1,3,5-triaza-7-phosphaadamantane, have shown very promising activity[70] and lead the way to the development of the RAPTA (Ru-Arene-PTA) species.

Cathepsin B is an ubiquitously expressed cysteine peptidase of the papain family, and has been proposed as tumor marker.[71] The exact role of cathepsin B in cancer has not been determined completely, but it is probably involved in tumor progression and metathesis.[72] Therefore, cathepsin B is a possible target for the control of tumor growth and it is inhibited by many metal complexes.[73]

RAPTA-pentaOH, where the η^6-arene is 5-phenyl-1-pentanol, is one of the most effective inhibitors of cathepsin B,[74] and this suggests a strong interaction with the protein. In the literature it was suggested that only one chloride ion undergoes aquation,[74-75] even if the loss

of both Cl^- cannot be excluded as demonstrated for other dichloro species such as Cp_2VCl_2.[10b, 26, 76] To show the possibility of the docking strategy presented here, the binding of RAPTA-pentaOH with cathepsin B was studied considering the release of only one or two chloride ligands. The calculations were carried out using the apo structure of the protein available in the Protein Data Bank (PDB code: 2ipp [77]), while the coordinates of metal complex were obtained from Cambridge Structural Database (CSD code: CUQCAT [74]). Before the docking, the protein was cleaned and the Ru species was activated in one or two positions occupied by Cl^- anions. Two evaluation spheres were built with a radius of 20 Å, centred respectively on the Cys29 and Cys237, the only two free cysteine residues of the protein. To take into account the side chain flexibility in solution, the Gold rotamer libraries[33] were applied to Cys29, Cys238 and the neighbors Gln237, Tyr177, His11, His199 and His239.

Two different interaction modes must be discussed: since RAPTA-pentaOH complex has two labile chloride ligands, one (first case, Figure 7) or both (second case, Figure 8) could be replaced by the amino acid side chain donors of cathepsin B. In the first case, the results show the presence of three potential binding sites: the interaction with S donor of Cys29 (56.29 GoldScore *Fitness* units, F_{max}), and the imidazole N of His190 and His239 (with score of 52.46 and 49.68); the predicted bond lengths Ru–S(Cys29), Ru–N(His190) and Ru–N(His239) are 2.255, 2.775 and 2.481 Å, respectively (the three binding sites, the amino acid involved in the direct coordination and second sphere stabilization are shown in Figure 7).

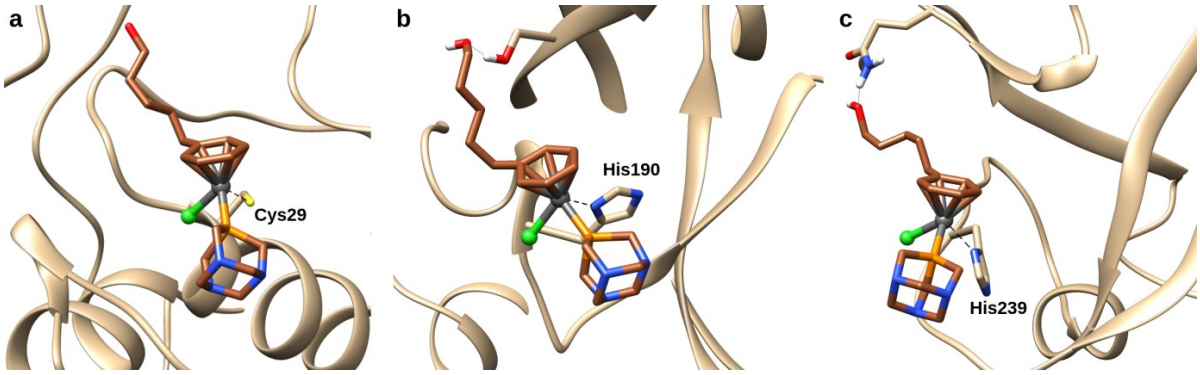

Figure 7. The three binding sites proposed by docking calculations for the interaction of RAPTA-pentaOH with cathepsin B after the aquation of only one labile chloride ligand: a) binding site with the coordination of Cys29; b) binding sites with the coordination of His190 and c) binding sites with the coordination of His239. The hydrogen bonds are highlighted with the full line.

In the second case, two potential binding sites were highlighted: one major site (F_{max} = 62.98), in which the metal is coordinated by S(Cys29) and CO(Gly198), and one secondary site (with GoldScore *Fitness* units of 54.46) that is characterized by the coordination of His239 with the second position remaining vacant; the predicted bond lengths Ru–S(Cys29) and Ru–O(Gly198) are 2.356 and 3.049 Å, while the distance Ru–N(His239) in the second site is 2.480 Å, very close to that found in the first case with only one free site. The results are represented in Figure 9.

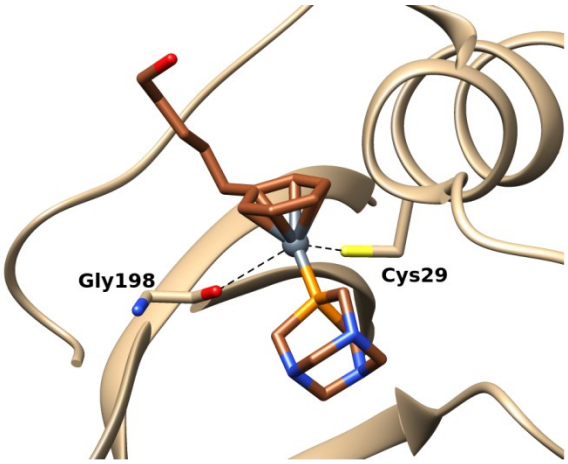

Figure 8. The three binding sites proposed by docking calculations for the interaction of RAPTA-pentaOH with cathepsin B after the aquation of both the labile chloride ligands. The adduct is formed after the exchange of two labile chloride ligands with Cys29 and CO group of Gly198.

The two interaction regions are shown in Figure 9. The role of Cys29 in the binding of Ru^{II} compounds with cathepsin B has been already discussed in the literature,[74,78] even if – in contrast with the previous papers – the proposed stabilization through hydrogen contacts with Glu72, His108 and His109 is not predicted in this study. However, the docking results suggest that a second binding region with the possible involvement of His190 and His239 residues could exist.

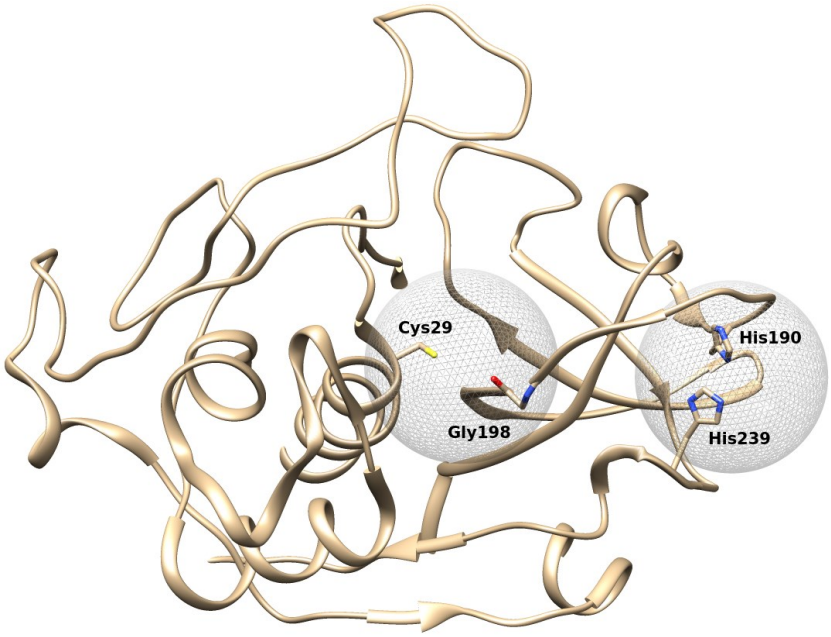

Figure 9. The two identified binding regions (primary binding site with Cys29 and Gly198, and secondary binding site with His190 and His239) of cathepsin B involved in Ru coordination are shown.

Conclusions

In our intents to bring dockings as a fundamental tool in the prediction of biometallic interactions, we here present a two sided study where a novel parametrization scheme is first tested against a series of twenty-five well characterized crystal structures in which a metal complex is bound to a protein with multiple coordination bonds ~~vacancies~~. In front of the results obtained, we extended the work to use it as a predictive tool for five different ~~systems~~ metallodrug-protein complexes for which X-ray structures are not available. The results indicate that our updated docking methodology is indeed an interesting and generalizable tool for the prediction of 3D models of the binding of metal complexes to proteins; in particular, i) the site of interaction and donors bound to metal are always successfully predicted and ii) after the recognition of the binding site the prediction ~~description~~ can be achieved ~~improved~~

taking into account the flexibility of the side chains located in the metal environment through the Gold rotamer libraries.

The application to metallodrugs interaction with proteins suggests binding modes in good agreement with the partial spectroscopic and spectrometric information available in the literature and proves useful to find additional hypotheses. In particular, the possibility of multiple coordination and stabilization through secondary interactions – hardly demonstrable with most of experimental techniques (ESI-MS, CD and UV-Vis) – can be substantiated by docking methods. A possible improvement of the bond distances and angles could be obtained through the refinement of the metal binding sites predicted by docking using QM/MM method.[7, 14]

We believe that the approach here reported, in combination with spectroscopic techniques or any experimental evidence, is easily expandable to other metal complexes and metallodrugs and could open major avenues in structural drug design and in the study of metal-proteins interaction.

Acknowledgments

J-D.M. and G.S. thank the Spanish grant CTQ2017-87889-P and Generalitat de Catalunya 2017SGR1323 and COST Action CM1306. G.S. is grateful also to the Universitat Autònoma de Barcelona for the support to his Ph.D. E.G. thank Fondazione di Sardegna (project FDS15Garribba) and FFABR 2017 "Fondo per il finanziamento delle attività base di ricerca" for the financial support.

Supporting Information

Equations for RMSD, APD and MAPD calculation, tables with information on the 25 X-ray crystallographic structures studied and results of the docking calculations (Table S1), docking results for the prediction of the binding site of $[Cu^{II}(Br)(L)(indazole)]$ to HSA, $V^{IV}O^{2+}$ to carboxypeptidase and oxalilplatin to ubiquitin (Tables S2-S4), Pt force field (Table S5) and Cartesian coordinates in PDB format of the calculated structures.

Author Information

Corresponding Authors

*E-mail: garribba@uniss.it (E.G.)

*E-mail: jeandidier.marechal@uab.cat (J-D.M.)

ORCID

Giuseppe Sciortino: 0000-0001-9657-1788

Eugenio Garribba: 0000-0002-7229-5966

Jean-Didier Maréchal: 0000-0002-8344-9043

Notes

The authors declare no competing financial interest.

References

(1) Rehder, D. *Bioinorganic Chemistry*. Oxford University Press: Oxford, 2014.

(2) (a) Guo, Z.; Sadler, P. J. Metals in Medicine. *Angew. Chem., Int. Ed.* **1999**, *38*, 1512-1537. (b) Farrell, N. Metal Complexes as Drugs and Chemotherapeutic Agents. In *Comprehensive Coordination Chemistry II*; McCleverty, J. A., Meyer, T. J., Ed.; Pergamon: Oxford, 2003; Vol. 9, pp 809-840. (c) Thompson, K. H. Medicinal Inorganic Chemistry: An Introduction. In *Encyclopedia of Inorganic and Bioinorganic Chemistry*; King, R. B., Ed.; John Wiley & Sons, Ltd: Chichester, 2011. (d) Barry, N. P. E.; Sadler, P. J. Exploration of the medical periodic table: towards new targets. *Chem. Commun.* **2013**, *49*, 5106-5131. (e) Mjos, K. D.; Orvig, C. Metallodrugs in Medicinal Inorganic Chemistry. *Chem. Rev.* **2014**, *114*, 4540-4563. (f) Medici, S.; Peana, M.; Nurchi, V. M.; Lachowicz, J. I.; Crisponi, G.; Zoroddu, M. A. Noble metals in medicine: Latest advances. *Coord. Chem. Rev.* **2015**, *284*, 329-350. (g) Zhang, P.; Sadler, P. J. Advances in the design of organometallic anticancer complexes. *J. Organomet. Chem.* **2017**, *839*, 5-14.

(3) (a) Jones, C.; Thornback, J. *Medicinal Applications of Coordination Chemistry*. The Royal Society of Chemistry: Cambridge, 2007. (b) *Metallotherapeutic Drugs and Metal-Based Diagnostic Agents. The Use of Metals in Medicine*. Gielen, M.; Tiekink, E. R. T., Eds. John Wiley & Sons Ltd: Chichester, 2005. (c) Dabrowiak, J. C. *Metals in Medicine*. John Wiley & Sons, Ltd: Chichester, 2009. (d) *Bioinorganic Medicinal Chemistry*. Alessio, E., Ed. Wiley-VCH Verlag GmbH & Co. KGaA: Weinheim, 2011. (e) *Interrelations between Essential Metal Ions and Human Diseases*. Springer Science+Business Media: Dordrecht, 2013.

(4) (a) Gumerova, N.; Krivosudský, L.; Fraqueza, G.; Breibeck, J.; Al-Sayed, E.; Tanuhadi, E.; Bijelic, A.; Fuentes, J.; Aureliano, M.; Rompel, A. The P-type ATPase inhibiting potential of polyoxotungstates. *Metallomics* **2018**, *10*, 287-295. (b) Bijelic, A.; Aureliano, M.; Rompel, A. The antibacterial activity of polyoxometalates: structures, antibiotic effects and future perspectives. *Chem. Commun.* **2018**, *54*, 1153-1169. (c) Bijelic, A.; Aureliano, M.; Rompel, A. Polyoxometalates as potential next-generation metallodrugs in the combat against cancer. *Angew. Chem., Int. Ed.* **2018**, DOI: 10.1002/anie.201803868.

(5) In docking terminology the species that interacts with the protein is named ligand. This term could generate confusion if the ligand is a metal complex; therefore, when it refers to the therminology used in the docking studies, it is written in italic in the text.

(6) Streib, M.; Kräling, K.; Richter, K.; Xie, X.; Steuber, H.; Meggers, E. An Organometallic Inhibitor for the Human Repair Enzyme 7,8-Dihydro-8-oxoguanosine Triphosphatase. *Angew. Chem., Int. Ed.* **2014**, *53*, 305-309.

(7) Robles, V. M.; Ortega-Carrasco, E.; Fuentes, E. G.; Lledos, A.; Marechal, J.-D. What can molecular modelling bring to the design of artificial inorganic cofactors? *Faraday Discuss.* **2011**, *148*, 137-159.

(8) (a) Neese, F. Quantum chemical calculations of spectroscopic properties of metalloproteins and model compounds: EPR and Mössbauer properties. *Curr. Opin. Chem. Biol.* **2003**, *7*, 125-135. (b) Neese, F. A critical evaluation of DFT, including time-dependent DFT, applied to bioinorganic chemistry. *J. Biol. Inorg. Chem.* **2006**, *11*, 702-711. (c) *Computational Inorganic and Bioinorganic Chemistry*. Solomon, E. I.; Scott, R. A.; King, R. B., Eds. John Wiley & Sons, Ltd: Chichester, 2009.

(9) (a) Warren, G. L.; Andrews, C. W.; Capelli, A.-M.; Clarke, B.; LaLonde, J.; Lambert, M. H.; Lindvall, M.; Nevins, N.; Semus, S. F.; Senger, S.; Tedesco, G.; Wall, I. D.; Woolven, J. M.; Peishoff, C. E.; Head, M. S. A Critical Assessment of Docking Programs and Scoring Functions. *J. Med. Chem.* **2006**, *49*, 5912-5931. (b) Xuan-Yu, M.; Hong-Xing, Z.; Mihaly, M.; Meng, C. Molecular Docking: A Powerful Approach for Structure-Based Drug Discovery. *Curr. Comput.-Aided Drug Des.* **2011**, *7*, 146-157. (c) Guedes, I. A.; de Magalhães, C. S.; Dardenne, L. E. Receptor–ligand molecular docking. *Biophys. Rev.* **2014**, *6*, 75-87. (d) Yuriev, E.; Holien, J.; Ramsland, P. A. Improvements, trends, and new ideas in molecular docking: 2012–2013 in review. *J. Mol. Recognit.* **2015**, *28*, 581-604. (e) Muñoz Robles, V.; Ortega-Carrasco, E.; Alonso-Cotchico, L.; Rodriguez-Guerra, J.; Lledós, A.; Maréchal, J.-D. Toward the Computational Design of Artificial Metalloenzymes: From Protein–Ligand Docking to Multiscale Approaches. *ACS Catalysis* **2015**, *5*, 2469-2480. (f) Akhter, M. Challenges in Docking: Mini Review. *JSM Chem.* **2016**, *4*, 1025. (g) Agarwal, S.; Mehrotra, R. An overview of Molecular Docking. *JSM Chem.* **2016**, *4*, 1024. (h) Wang, G.; Zhu, W. Molecular docking for drug discovery and development: a widely used approach but far from perfect. *Future Med. Chem.* **2016**, *8*, 1707-1710.

(10) (a) Wang, Z.; Sun, H.; Yao, X.; Li, D.; Xu, L.; Li, Y.; Tian, S.; Hou, T. Comprehensive evaluation of ten docking programs on a diverse set of protein–ligand complexes: the prediction accuracy of sampling power and scoring power. *Phys. Chem. Chem. Phys.* **2016**, *18*, 12964-12975. (b) Wang, Z.; Kang, Y.; Li, D.; Sun, H.; Dong, X.; Yao, X.; Xu, L.; Chang, S.; Li, Y.; Hou, T. Benchmark Study Based on 2P2IDB to Gain Insights into the Discovery of Small-Molecule PPI Inhibitors. *J. Phys. Chem. B* **2018**, *122*, 2544-2555.

(11) Sousa, S. F.; Ribeiro, A. J. M.; Coimbra, J. T. S.; Neves, R. P. P.; Martins, S. A.; Moorthy, N. S. H. N.; Fernandes, P. A.; Ramos, M. J. Protein-Ligand Docking in the New Millennium – A Retrospective of 10 Years in the Field. *Curr. Med. Chem.* **2013**, *20*, 2296-2314.

(12) Pagadala, N. S.; Syed, K.; Tuszynski, J. Software for molecular docking: a review. *Biophysical Reviews* **2017**, *9*, 91-102.

(13) Riccardi, L.; Genna, V.; De Vivo, M. Metal–ligand interactions in drug design. *Nature Reviews Chemistry* **2018**, *2*, 100-112.

(14) Ortega-Carrasco, E.; Lledós, A.; Maréchal, J.-D. Unravelling novel synergies between organometallic and biological partners: a quantum mechanics/molecular mechanics study of an artificial metalloenzyme. *J. R. Soc. Interface* **2014**, *11*, 20140090.

(15) Sciortino, G.; Sanna, D.; Ugone, V.; Lledós, A.; Maréchal, J.-D.; Garribba, E. Decoding Surface Interaction of $V^{IV}O$ Metallodrug Candidates with Lysozyme. *Inorg. Chem.* **2018**, *57*, 4456-4469.

(16) (a) Jones, G.; Willett, P.; Glen, R. C.; Leach, A. R.; Taylor, R. Development and validation of a genetic algorithm for flexible docking1. *J. Mol. Biol.* **1997**, *267*, 727-748. (b) Verdonk, M. L.; Cole, J. C.; Hartshorn, M. J.; Murray, C. W.; Taylor, R. D. Improved protein–ligand docking using GOLD. *Proteins: Struct., Funct., Bioinf.* **2003**, *52*, 609-623.

(17) (a) Morris, G. M.; Huey, R.; Lindstrom, W.; Sanner, M. F.; Belew, R. K.; Goodsell, D. S.; Olson, A. J. AutoDock4 and AutoDockTools4: Automated Docking with Selective Receptor Flexibility. *J. Comput. Chem.* **2009**, *30*, 2785-2791. (b) Santos-Martins, D.; Forli, S.; Ramos, M. J.; Olson, A. J. AutoDock4Zn: An Improved AutoDock Force Field for Small-Molecule Docking to Zinc Metalloproteins. *J. Chem. Inf. Model.* **2014**, *54*, 2371-2379.

(18) Ouyang, X.; Zhou, S.; Su, C. T. T.; Ge, Z.; Li, R.; Kwoh, C. K. CovalentDock: Automated covalent docking with parameterized covalent linkage energy estimation and molecular geometry constraints. *J. Comput. Chem.* **2013**, *34*, 326-336.

(19) Scholz, C.; Knorr, S.; Hamacher, K.; Schmidt, B. DOCKTITE–A Highly Versatile Step-by-Step Workflow for Covalent Docking and Virtual Screening in the Molecular Operating Environment. *J. Chem. Inf. Model.* **2015**, *55*, 398-406.

(20) Sciortino, G.; Sanna, D.; Ugone, V.; Micera, G.; Lledós, A.; Maréchal, J.-D.; Garribba, E. Elucidation of Binding Site and Chiral Specificity of Oxidovanadium Drugs with Lysozyme through Theoretical Calculations. *Inorg. Chem.* **2017**, *56*, 12938-12951.

(21) Sciortino, G.; Rodríguez-Guerra Pedregal, J.; Lledós, A.; Garribba, E.; Maréchal, J.-D. Prediction of the interaction of metallic moieties with proteins: an update for protein-ligand docking techniques. *J. Comput. Chem.* **2018**, *39*, 42-51.

(22) Gou, Y.; Qi, J.; Ajayi, J.-P.; Zhang, Y.; Zhou, Z.; Wu, X.; Yang, F.; Liang, H. Developing Anticancer Copper(II) Pro-drugs Based on the Nature of Cancer Cells and the Human Serum Albumin Carrier IIA Subdomain. *Mol. Pharm.* **2015**, *12*, 3597-3609.

(23) DeKoch, R. J.; West, D. J.; Cannon, J. C.; Chasteen, N. D. Kinetics and electron paramagnetic resonance spectra of vanadyl(IV) carboxypeptidase A. *Biochemistry* **1974**, *13*, 4347-4354.

(24) Sanna, D.; Pecoraro, V. L.; Micera, G.; Garribba, E. Application of DFT methods to the study of the coordination environment of the VO^{2+} ion in V proteins. *J. Biol. Inorg. Chem.* **2012**, *17*, 773-790.

(25) (a) Finkelstein, A. E.; Walz, D. T.; Batista, V.; Mizraji, M.; Roisman, F.; Misher, A. Auranofin. New oral gold compound for treatment of rheumatoid arthritis. *Ann. Rheum. Dis.* **1976**, *35*, 251-257. (b) Shaw, C. F. Gold-Based Therapeutic Agents. *Chem. Rev.* **1999**, *99*, 2589-2600.

(26) Qureshi, I. A.; Ferron, F.; Seh, C. C.; Cheung, P.; Lescar, J. Crystallographic structure of ubiquitin in complex with cadmium ions. *BMC Research Notes* **2009**, *2*, 251.

(27) (a) Greenwood, N. N.; Earnshaw, A. *Chemistry of the Elements*. Butterworth-Heinemann: Oxford, 1997. (b) Frausto da Silva, J. J. R.; Williams, R. J. P. *The Biological Chemistry of the Elements: The Inorganic Chemistry of Life*. Oxford University Press: Oxford, 2001. (c) *Biochemistry of the Essential Ultratrace Elements*. Frieden, E., Ed. Plenum Press: New York, 2012. (d) Crichton, R. *Biological Inorganic Chemistry. A New Introduction to Molecular Structure and Function. 2nd Edition*. Elsevier: Oxford, 2012. (e) *Comprehensive Inorganic Chemistry II. From Elements to Applications, 2nd Ed.* Reedijk, J.; Poeppelmeier, K., Eds. Elsevier: Amsterdam, 2013. (f) *Binding, Transport and Storage of Metal Ions in Biological Cells*. Maret, W.; Wedd, A., Eds. The Royal Society of Chemistry: Cambridge, 2014.

(28) (a) Burley, S. K.; Berman, H. M.; Christie, C.; Duarte, J. M.; Feng, Z.; Westbrook, J.; Young, J.; Zardecki, C. RCSB Protein Data Bank: Sustaining a living digital data resource that enables breakthroughs in scientific research and biomedical education. *Protein Sci.* **2018**, *27*, 316-330. (b) Rose, P. W.; Prlić, A.; Altunkaya, A.; Bi, C.; Bradley, A. R.; Christie, C. H.; Costanzo, L. D.; Duarte, J. M.; Dutta, S.; Feng, Z.; Green, R. K.; Goodsell, D. S.; Hudson, B.; Kalro, T.; Lowe, R.; Peisach, E.; Randle, C.; Rose, A. S.; Shao, C.; Tao, Y.-P.; Valasatava,

Y.; Voigt, M.; Westbrook, J. D.; Woo, J.; Yang, H.; Young, J. Y.; Zardecki, C.; Berman, H. M.; Burley, S. K. The RCSB protein data bank: integrative view of protein, gene and 3D structural information. *Nucleic Acids Res.* **2017**, *45*, D271-D281. (c) Berman, H. M.; Westbrook, J.; Feng, Z.; Gilliland, G.; Bhat, T. N.; Weissig, H.; Shindyalov, I. N.; Bourne, P. E. The Protein Data Bank. *Nucleic Acids Res.* **2000**, *28*, 235-242.

(29) Groom, C. R.; Bruno, I. J.; P., L. M.; Ward, S. C. The Cambridge Structural Database. *Acta Crystallogr., Sect. B: Struct. Sci.* **2016**, *B72*, 171-179.

(30) Pettersen, E. F.; Goddard, T. D.; Huang, C. C.; Couch, G. S.; Greenblatt, D. M.; Meng, E. C.; Ferrin, T. E. UCSF Chimera-A visualization system for exploratory research and analysis. *J. Comput. Chem.* **2004**, *25*, 1605-1612.

(31) Jones, G.; Willett, P.; Glen, R. C. Molecular recognition of receptor sites using a genetic algorithm with a description of desolvation. *J. Mol. Biol.* **1995**, *245*, 43-53.

(32) Sanna, D.; Ugone, V.; Sciortino, G.; Buglyo, P.; Bihari, Z.; Parajdi-Losonczi, P. L.; Garribba, E. $V^{IV}O$ complexes with antibacterial quinolone ligands and their interaction with serum proteins. *Dalton Trans.* **2018**, *47*, 2164-2182.

(33) Lovell, S. C.; Word, J. M.; Richardson, J. S.; Richardson, D. C. The penultimate rotamer library. *Proteins: Struct., Funct., Bioinf.* **2000**, *40*, 389-408.

(34) (a) Rodríguez-Guerra, J. *Insilichem/gaudiview: Pre-alpha public releas, Zenodo*. 2017. (b) Rodríguez-Guerra Pedregal, J.; Sciortino, G.; Guasp, J.; Municoy, M.; Maréchal, J.-D. GaudiMM: A modular multi-objective platform for molecular modeling. *J. Comput. Chem.* **2017**, *38*, 2118-2126.

(35) (a) Bijelic, A.; Theiner, S.; Keppler, B. K.; Rompel, A. X-ray Structure Analysis of Indazolium *trans*-[Tetrachlorobis(1*H*-indazole)ruthenate(III)] (KP1019) Bound to Human Serum Albumin Reveals Two Ruthenium Binding Sites and Provides Insights into the Drug Binding Mechanism. *J. Med. Chem.* **2016**, *59*, 5894-5903. (b) Lubkowski, J.; Yang, F.; Alexandratos, J.; Wlodawer, A.; Zhao, H.; Burke, T. R., Jr.; Neamati, N.; Pommier, Y.; Merkel, G.; Skalka, A. M. Structure of the catalytic domain of avian sarcoma virus integrase with a bound HIV-1 integrase-targeted inhibitor. *Proc. Natl. Acad. Sci. U. S. A.* **1998**, *95*, 4831-4836. (c) Ohlendorf, D. H.; Orville, A. M.; Lipscomb, J. D. Structure of protocatechuate 3,4-dioxygenase from Pseudomonas aeruginosa at 2.15 A resolution. *J. Mol. Biol.* **1994**, *244*, 586-608. (d) *Structural Modification of the hydrophobic pocket in Human Carbonic Anhydrase II*. http://www.rcsb.org/pdb/explore/explore.do?structureId=3U45. (e) *Structural insights into protein splicing inhibition by platinum therapeutics as potential anti-microbials*. http://www.rcsb.org/pdb/explore/explore.do?structureId=5I0A. (f) Wilkinson, D.; Akumanyi,

N.; Hurtado-Guerrero, R.; Dawkes, H.; Knowles, P. F.; Phillips, S. E.; McPherson, M. J. Structural and kinetic studies of a series of mutants of galactose oxidase identified by directed evolution. *Protein engineering, design & selection : PEDS* **2004**, *17*, 141-148. (g) Ang, W. H.; Parker, L. J.; De Luca, A.; Juillerat-Jeanneret, L.; Morton, C. J.; Lo Bello, M.; Parker, M. W.; Dyson, P. J. Rational design of an organometallic glutathione transferase inhibitor. *Angew. Chem. Int. Ed. Engl.* **2009**, *48*, 3854-3857. (h) Herzberg, O.; Chen, C. C.; Liu, S.; Tempczyk, A.; Howard, A.; Wei, M.; Ye, D.; Dunaway-Mariano, D. Pyruvate site of pyruvate phosphate dikinase: crystal structure of the enzyme-phosphonopyruvate complex, and mutant analysis. *Biochemistry* **2002**, *41*, 780-787. (i) *Metal exchange in thermolysin*. http://www.rcsb.org/pdb/explore/explore.do?structureId=3FXS. (j) Messori, L.; Marzo, T.; Merlino, A. Interactions of carboplatin and oxaliplatin with proteins: Insights from X-ray structures and mass spectrometry studies of their ribonuclease A adducts. *J. Inorg. Biochem.* **2015**, *153*, 136-142. (k) Vergara, A.; D'Errico, G.; Montesarchio, D.; Mangiapia, G.; Paduano, L.; Merlino, A. Interaction of anticancer ruthenium compounds with proteins: high-resolution X-ray structures and raman microscopy studies of the adduct between hen egg white lysozyme and AziRu. *Inorg. Chem.* **2013**, *52*, 4157-4159. (l) Shirataki, C.; Shoji, O.; Terada, M.; Ozaki, S.; Sugimoto, H.; Shiro, Y.; Watanabe, Y. Inhibition of heme uptake in Pseudomonas aeruginosa by its hemophore (HasA(p)) bound to synthetic metal complexes. *Angew. Chem. Int. Ed. Engl.* **2014**, *53*, 2862-2866. (m) Krieg, S.; Huche, F.; Diederichs, K.; Izadi-Pruneyre, N.; Lecroisey, A.; Wandersman, C.; Delepelaire, P.; Welte, W. Heme uptake across the outer membrane as revealed by crystal structures of the receptor-hemophore complex. *Proc. Natl. Acad. Sci. U. S. A.* **2009**, *106*, 1045-1050. (n) Qi, J.; Gou, Y.; Zhang, Y.; Yang, K.; Chen, S.; Liu, L.; Wu, X.; Wang, T.; Zhang, W.; Yang, F. Developing Anticancer Ferric Prodrugs Based on the N-Donor Residues of Human Serum Albumin Carrier IIA Subdomain. *J. Med. Chem.* **2016**, *59*, 7497-7511. (o) Katz, B. A.; Clark, J. M.; Finer-Moore, J. S.; Jenkins, T. E.; Johnson, C. R.; Ross, M. J.; Luong, C.; Moore, W. R.; Stroud, R. M. Design of potent selective zinc-mediated serine protease inhibitors. *Nature* **1998**, *391*, 608-612. (p) Balakrishnan, R.; Ramasubbu, N.; Varughese, K. I.; Parthasarathy, R. Crystal structures of the copper and nickel complexes of RNase A: metal-induced interprotein interactions and identification of a novel copper binding motif. *Proc. Natl. Acad. Sci. U. S. A.* **1997**, *94*, 9620-9625. (q) Fusetti, F.; Schroter, K. H.; Steiner, R. A.; van Noort, P. I.; Pijning, T.; Rozeboom, H. J.; Kalk, K. H.; Egmond, M. R.; Dijkstra, B. W. Crystal structure of the copper-containing quercetin 2,3-dioxygenase from Aspergillus japonicus. *Structure* **2002**, *10*, 259-268. (r) Han, S.; Eltis, L. D.; Timmis, K. N.; Muchmore, S. W.; Bolin, J. T. Crystal

structure of the biphenyl-cleaving extradiol dioxygenase from a PCB-degrading pseudomonad. *Science* **1995**, *270*, 976-980. (s) Munoz, I. G.; Moran, J. F.; Becana, M.; Montoya, G. The crystal structure of an eukaryotic iron superoxide dismutase suggests intersubunit cooperation during catalysis. *Protein Sci.* **2005**, *14*, 387-394. (t) Perry, J. J.; Hearn, A. S.; Cabelli, D. E.; Nick, H. S.; Tainer, J. A.; Silverman, D. N. Contribution of human manganese superoxide dismutase tyrosine 34 to structure and catalysis. *Biochemistry* **2009**, *48*, 3417-3424. (u) Ferraro, G.; Ciambellotti, S.; Messori, L.; Merlino, A. Cisplatin Binding Sites in Human H-Chain Ferritin. **2017**, *56*, 9064-9070.

(36) (a) Tisato, F.; Marzano, C.; Porchia, M.; Pellei, M.; Santini, C. Copper in diseases and treatments, and copper-based anticancer strategies. *Med. Res. Rev.* **2010**, *30*, 708-749. (b) Santini, C.; Pellei, M.; Gandin, V.; Porchia, M.; Tisato, F.; Marzano, C. Advances in Copper Complexes as Anticancer Agents. *Chem. Rev.* **2014**, *114*, 815-862. (c) Hordyjewska, A.; Popiołek, Ł.; Kocot, J. The many "faces" of copper in medicine and treatment. *BioMetals* **2014**, *27*, 611-621. (d) Tabti, R.; Tounsi, N.; Gaiddon, C.; Bentouhami, E.; Désaubry, L. Progress in Copper Complexes as Anticancer Agents. *Med. Chem.* **2017**, *7*, 139-143. (e) Acilan, C.; Cevatemre, B.; Adiguzel, Z.; Karakas, D.; Ulukaya, E.; Ribeiro, N.; Correia, I.; Pessoa, J. C. Synthesis, biological characterization and evaluation of molecular mechanisms of novel copper complexes as anticancer agents. *Biochimica et Biophysica Acta (BBA) - General Subjects* **2017**, *1861*, 218-234. (f) Mahendiran, D.; Amuthakala, S.; Bhuvanesh, N. S. P.; Kumar, R. S.; Rahiman, A. K. Copper complexes as prospective anticancer agents: in vitro and in vivo evaluation, selective targeting of cancer cells by DNA damage and S phase arrest. *RSC Advances* **2018**, *8*, 16973-16990.

(37) (a) Kratz, F. Albumin as a drug carrier: Design of prodrugs, drug conjugates and nanoparticles. *J. Control. Release* **2008**, *132*, 171-183. (b) Elsadek, B.; Kratz, F. Impact of albumin on drug delivery – New applications on the horizon. *J. Control. Release* **2012**, *157*, 4-28. (c) Kratz, F.; Elsadek, B. Clinical impact of serum proteins on drug delivery. *J. Control. Release* **2012**, *161*, 429-445. (d) Kratz, F. A clinical update of using albumin as a drug vehicle – A commentary. *J. Control. Release* **2014**, *190*, 331-336.

(38) Curry, S.; Mandelkow, H.; Brick, P.; Franks, N. Crystal structure of human serum albumin complexed with fatty acid reveals an asymmetric distribution of binding sites. *Nat. Struct. Mol. Biol.* **1998**, *5*, 827-835.

(39) Hathaway, B. J. Copper. In *Comprehensive Coordination Chemistry*; Wilkinson, G., Gillard, R. D., McCleverty, J. A., Ed.; Pergamon Press: Oxford, 1985; Vol. 5, pp 533-774.

(40) (a) Sakurai, H.; Kojima, Y.; Yoshikawa, Y.; Kawabe, K.; Yasui, H. Antidiabetic vanadium(IV) and zinc(II) complexes. *Coord. Chem. Rev.* **2002**, *226*, 187-198. (b) Thompson, K. H.; Orvig, C. Vanadium Compounds in the Treatment of Diabetes. In *Met. Ions Biol. Syst.*; Sigel, H., Sigel, A., Ed.; Marcel Dekker: New York, 2004; Vol. 41, pp 221-252. (c) Thompson, K. H.; Orvig, C. Vanadium in diabetes: 100 years from phase 0 to phase I. *J. Inorg. Biochem.* **2006**, *100*, 1925-1935. (d) Sakurai, H.; Yoshikawa, Y.; Yasui, H. Current state for the development of metallopharmaceutics and anti-diabetic metal complexes. *Chem. Soc. Rev.* **2008**, *37*, 2383-2392. (e) Thompson, K. H.; Lichter, J.; LeBel, C.; Scaife, M. C.; McNeill, J. H.; Orvig, C. Vanadium treatment of type 2 diabetes: A view to the future. *J. Inorg. Biochem.* **2009**, *103*, 554-558. (f) Rehder, D. The potentiality of vanadium in medicinal applications. *Future Med. Chem.* **2012**, *4*, 1823-1837. (g) Costa Pessoa, J.; Etcheverry, S.; Gambino, D. Vanadium compounds in medicine. *Coord. Chem. Rev.* **2015**, *301-302*, 24-48. (h) Rehder, D. Perspectives for vanadium in health issues. *Future Med. Chem.* **2016**, *8*, 325-338. (i) Rehder, D. Implications of vanadium in technical applications and pharmaceutical issues. *Inorg. Chim. Acta* **2017**, *455*, 378-389. (j) Jakusch, T.; Kiss, T. In vitro study of the antidiabetic behavior of vanadium compounds. *Coord. Chem. Rev.* **2017**, *351*, 118-126.

(41) (a) Kioseoglou, E.; Petanidis, S.; Gabriel, C.; Salifoglou, A. The chemistry and biology of vanadium compounds in cancer therapeutics. *Coord. Chem. Rev.* **2015**, 87-105. (b) Scalese, G.; Mosquillo, M. F.; Rostán, S.; Castiglioni, J.; Alho, I.; Pérez, L.; Correia, I.; Marques, F.; Costa Pessoa, J.; Gambino, D. Heteroleptic oxidovanadium(IV) complexes of 2-hydroxynaphtylaldimine and polypyridyl ligands against Trypanosoma cruzi and prostate cancer cells. *J. Inorg. Biochem.* **2017**, *175*, 154-166. (c) Crans, D., C; Yang, L.; Haase, A.; Yang, X. Health Benefits of Vanadium and Its Potential as an Anticancer Agent. In *Metal Ions in Life Sciences*; Sigel, A., H., S., Freisinger, E., Sigel, R. K. O., Ed.; De Gruyter GmbH: Berlin, 2018; Vol. 18, pp 251-279.

(42) Rehder, D. *Bioinorganic Vanadium Chemistry*. John Wiley & Sons, Ltd: Chichester, 2008.

(43) (a) Macara, I. G.; Kustin, K.; Cantley Jr, L. C. Glutathione reduces cytoplasmic vanadate mechanism and physiological implications. *Biochim. Biophys. Acta, Gen. Subj.* **1980**, *629*, 95-106. (b) Garner, M.; Reglinski, J.; Smith, W. E.; McMurray, J.; Abdullah, I.; Wilson, R. A ^{1}H spin echo and ^{51}V NMR study of the interaction of vanadate with intact erythrocytes. *J. Biol. Inorg. Chem.* **1997**, *2*, 235-241. (c) De Cremer, K.; Van Hulle, M.; Chéry, C.; Cornelis, R.; Strijckmans, K.; Dams, R.; Lameire, N.; Vanholder, R. Fractionation of vanadium complexes in serum, packed cells and tissues of Wistar rats by means of gel

filtration and anion-exchange chromatography. *J. Biol. Inorg. Chem.* **2002**, *7*, 884-890. (d) Delgado, T. C.; Tomaz, A. I.; Correia, I.; Costa Pessoa, J.; Jones, J. G.; Geraldes, C. F. G. C.; Castro, M. M. C. A. Uptake and metabolic effects of insulin mimetic oxovanadium compounds in human erythrocytes. *J. Inorg. Biochem.* **2005**, *99*, 2328-2339. (e) Sanna, D.; Serra, M.; Micera, G.; Garribba, E. Interaction of antidiabetic vanadium compounds with hemoglobin and red blood cells and their distribution between plasma and erythrocytes. *Inorg. Chem.* **2014**, *53*, 1449-1464.

(44) Rehder, D. The future of/for vanadium. *Dalton Trans.* **2013**, *42*, 11749-11761.

(45) Chasteen, D. N. Vanadium-protein interactions. In *Met. Ions Biol. Syst.*; Sigel, H., Sigel, A., Ed.; Marcel Dekker: New York, 1995; Vol. 31, pp 231-247.

(46) (a) Bertini, I.; Gray, H. B.; J., L. S.; S., V. J. *Bioinorganic Chemistry*. University Science Books: Mill Valley, California, 1994. (b) Lippard, S. J.; Berg, J. M. *Principles of bioinorganic chemistry*. University Science Books: Mill Valley, 1994.

(47) Bukrinsky, J. T.; Bjerrum, M. J.; Kadziola, A. Native Carboxypeptidase A in a New Crystal Environment Reveals a Different Conformation of the Important Tyrosine 248. *Biochemistry* **1998**, *37*, 16555-16564.

(48) Rees, D. C.; Lewis, M.; Lipscomb, W. N. Refined crystal structure of carboxypeptidase a at 1·54 Å resolution. *J. Mol. Biol.* **1983**, *168*, 367-387.

(49) Smith II, T. S.; Root, C. A.; Kampf, J. W.; Rasmussen, P. G.; Pecoraro, V. L. Reevaluation of the additivity relationship for vanadyl−imidazole complexes: Correlation of the EPR hyperfine constant with ring orientation. *J. Am. Chem. Soc.* **2000**, *122*, 767-775.

(50) Vilas Boas, L. F.; Costa Pessoa, J. Vanadium. In *Comprehensive Coordination Chemistry*; Wilkinson, G., Gillard, R. D., McCleverty, J. A., Ed.; Pergamon Press: Oxford, 1985; Vol. 3, pp 453-583.

(51) (a) Faa, G.; Gerosa, C.; Fanni, D.; Lachowicz, J. I.; Nurchi, V. M. Gold - Old Drug with New Potentials. *Curr. Med. Chem.* **2018**, *25*, 75-84. (b) Yeo, C.; Ooi, K.; Tiekink, E. Gold-Based Medicine: A Paradigm Shift in Anti-Cancer Therapy? *Molecules* **2018**, *23*, 1410. (c) Porchia, M.; Pellei, M.; Marinelli, M.; Tisato, F.; Del Bello, F.; Santini, C. New insights in Au-NHCs complexes as anticancer agents. *Eur. J. Med. Chem.* **2018**, *146*, 709-746.

(52) Identifier NCT01419691; Phase I and II Study of Auranofin in Chronic Lymphocytic Leukemia (CLL). https://clinicaltrials.gov/ct2/show/NCT01419691.

(53) Dean, T. C.; Yang, M.; Liu, M.; Grayson, J. M.; DeMartino, A. W.; Day, C. S.; Lee, J.; Furdui, C. M.; Bierbach, U. Human Serum Albumin-Delivered $[Au(PEt_3)]^+$ Is a Potent Inhibitor of T Cell Proliferation. *ACS Medicinal Chemistry Letters* **2017**, *8*, 572-576.

(54) Mirabell, C. K.; Johnson, R. K.; Hill, D. T.; Faucette, L. F.; Girard, G. R.; Kuo, G. Y.; Sung, C. M.; Crooke, S. T. Correlation of the in vitro cytotoxic and in vivo antitumor activities of gold(I) coordination complexes. *J. Med. Chem.* **1986**, *29*, 218-223.

(55) Sugio, S.; Kashima, A.; Mochizuki, S.; Noda, M.; Kobayashi, K. Crystal structure of human serum albumin at 2.5 Å resolution. *Protein Eng., Des. Sel.* **1999**, *12*, 439-446.

(56) Zou, J.; Taylor, P.; Dornan, J.; Robinson, S. P.; Walkinshaw, M. D.; Sadler, P. J. First Crystal Structure of a Medicinally Relevant Gold Protein Complex: Unexpected Binding of $[Au(PEt_3)]^+$ to Histidine. *Angew. Chem., Int. Ed.* **2000**, *39*, 2931-2934.

(57) Christodoulou, J.; Sadler, P. J.; Tucker, A. ^{1}H NMR of albumin in human blood plasma: drug binding and redox reactions at Cys34. *FEBS Lett.* **1995**, *376*, 1-5.

(58) Roberts, J. R.; Xiao, J.; Schliesman, B.; Parsons, D. J.; Shaw, C. F. Kinetics and Mechanism of the Reaction between Serum Albumin and Auranofin (and Its Isopropyl Analogue) in Vitro. *Inorg. Chem.* **1996**, *35*, 424-433.

(59) Coffer, M. T.; Shaw, C. F.; Eidsness, M. K.; Watkins, J. W.; Elder, R. C. Reactions of auranofin and chloro(triethylphosphine)gold with bovine serum albumin. *Inorg. Chem.* **1986**, *25*, 333-339.

(60) (a) Rosenberg, B.; Vancamp, L.; Trosko, J. E.; Mansour, V. H. Platinum Compounds: a New Class of Potent Antitumour Agents. *Nature* **1969**, *222*, 385-386. (b) Rosenberg, B.; VanCamp, L. The Successful Regression of Large Solid Sarcoma 180 Tumors by Platinum Compounds. *Cancer Res.* **1970**, *30*, 1799-1802.

(61) (a) Johnstone, T. C.; Suntharalingam, K.; Lippard, S. J. The Next Generation of Platinum Drugs: Targeted Pt(II) Agents, Nanoparticle Delivery, and Pt(IV) Prodrugs. *Chem. Rev.* **2016**, *116*, 3436-3486. (b) Oun, R.; Moussa, Y. E.; Wheate, N. J. The side effects of platinum-based chemotherapy drugs: a review for chemists. *Dalton Trans.* **2018**, *47*, 6645-6653. (c) Tylkowski, B.; Jastrząb, R.; Odani, A., Developments in platinum anticancer drugs. In *Physical Sciences Reviews*, 2018; Vol. 3.

(62) Kelland, L. The resurgence of platinum-based cancer chemotherapy. *Nat. Rev. Cancer* **2007**, *7*, 573-584.

(63) Graham, J.; Muhsin, M.; Kirkpatrick, P. Oxaliplatin. *Nat. Rev. Drug Discovery* **2004**, *3*, 11-12.

(64) Meier, S. M.; Tsybin, Y. O.; Dyson, P. J.; Keppler, B. K.; Hartinger, C. G. Fragmentation methods on the balance: unambiguous top–down mass spectrometric characterization of oxaliplatin–ubiquitin binding sites. *Anal. Bioanal. Chem.* **2012**, *402*, 2655-2662.

(65) (a) Popolin, C. P.; Cominetti, M. R. A Review of Ruthenium Complexes Activities on Breast Cancer Cells. *Mini reviews in medicinal chemistry* **2016**, *17*, 1435-1441. (b) Zeng, L.; Gupta, P.; Chen, Y.; Wang, E.; Ji, L.; Chao, H.; Chen, Z.-S. The development of anticancer ruthenium(ii) complexes: from single molecule compounds to nanomaterials. *Chem. Soc. Rev.* **2017**, *46*, 5771-5804. (c) Leon, I. E.; Cadavid-Vargas, J. F.; Di Virgilio, A. L.; Etcheverry, S. B. Vanadium, ruthenium and copper compounds: a new class of nonplatinum metallodrugs with anticancer activity. *Curr. Med. Chem.* **2017**, *24*, 112-148.

(66) (a) Leijen, S.; Burgers, S. A.; Baas, P.; Pluim, D.; Tibben, M.; van Werkhoven, E.; Alessio, E.; Sava, G.; Beijnen, J. H.; Schellens, J. H. M. Phase I/II study with ruthenium compound NAMI-A and gemcitabine in patients with non-small cell lung cancer after first line therapy. *Invest. New Drugs* **2015**, *33*, 201-214. (b) Rademaker-Lakhai, J. M.; van den Bongard, D.; Pluim, D.; Beijnen, J. H.; Schellens, J. H. M. A Phase I and Pharmacological Study with Imidazolium-*trans*-DMSO-imidazole-tetrachlororuthenate, a Novel Ruthenium Anticancer Agent. *Clinical Cancer Research* **2004**, *10*, 3717-3727.

(67) Hartinger, C. G.; Zorbas-Seifried, S.; Jakupec, M. A.; Kynast, B.; Zorbas, H.; Keppler, B. K. From bench to bedside – preclinical and early clinical development of the anticancer agent indazolium *trans*-[tetrachlorobis(1H-indazole)ruthenate(III)] (KP1019 or FFC14A). *J. Inorg. Biochem.* **2006**, *100*, 891-904.

(68) Sava, G.; Bergamo, A.; Zorzet, S.; Gava, B.; Casarsa, C.; Cocchietto, M.; Furlani, A.; Scarcia, V.; Serli, B.; Iengo, E.; Alessio, E.; Mestroni, G. Influence of chemical stability on the activity of the antimetastasis ruthenium compound NAMI-A. *Eur. J. Cancer* **2002**, *38*, 427-435.

(69) Dyson, P. J.; Sava, G. Metal-based antitumour drugs in the post genomic era. *Dalton Trans.* **2006**, 1929-1933.

(70) Scolaro, C.; Bergamo, A.; Brescacin, L.; Delfino, R.; Cocchietto, M.; Laurenczy, G.; Geldbach, T. J.; Sava, G.; Dyson, P. J. In Vitro and in Vivo Evaluation of Ruthenium(II)−Arene PTA Complexes. *J. Med. Chem.* **2005**, *48*, 4161-4171.

(71) Gondi, C. S.; Rao, J. S. Cathepsin B as a cancer target. *Expert Opinion on Therapeutic Targets* **2013**, *17*, 281-291.

(72) (a) Podgorski, I.; Sloane, B. F. Cathepsin B and its role(s) in cancer progression. *Biochem. Soc. Symp.* **2003**, *70*, 263-276. (b) Mohamed, M. M.; Sloane, B. F. multifunctional enzymes in cancer. *Nat. Rev. Cancer* **2006**, *6*, 764-775.

(73) (a) Fricker, S. P. Cysteine proteases as targets for metal-based drugs. *Metallomics* **2010**, *2*, 366-377. (b) Kilpin, K. J.; Dyson, P. J. Enzyme inhibition by metal complexes: concepts, strategies and applications. *Chem. Sci.* **2013**, *4*, 1410-1419.

(74) Casini, A.; Gabbiani, C.; Sorrentino, F.; Rigobello, M. P.; Bindoli, A.; Geldbach, T. J.; Marrone, A.; Re, N.; Hartinger, C. G.; Dyson, P. J.; Messori, L. Emerging Protein Targets for Anticancer Metallodrugs: Inhibition of Thioredoxin Reductase and Cathepsin B by Antitumor Ruthenium(II)−Arene Compounds. *J. Med. Chem.* **2008**, *51*, 6773-6781.

(75) Berger, I.; Hanif, M.; Nazarov, A. A.; Hartinger, C. G.; John, R. O.; Kuznetsov, M. L.; Groessl, M.; Schmitt, F.; Zava, O.; Biba, F.; Arion, V. B.; Galanski, M.; Jakupec, M. A.; Juillerat-Jeanneret, L.; Dyson, P. J.; Keppler, B. K. In Vitro Anticancer Activity and Biologically Relevant Metabolization of Organometallic Ruthenium Complexes with Carbohydrate-Based Ligands. *Chem.–Eur. J.* **2008**, *14*, 9046-9057.

(76) Toney, J. H.; Brock, C. P.; Marks, T. J. Aqueous coordination chemistry of vanadocene dichloride with nucleotides and phosphoesters. Mechanistic implications for a new class of antitumor agents. *J. Am. Chem. Soc.* **1986**, *108*, 7263-7274.

(77) Huber, C. P.; Campbell, R. L.; Hasnain, S.; Hirama, T.; To, R., results not yet published.

(78) Ciancetta, A.; Genheden, S.; Ryde, U. A QM/MM study of the binding of RAPTA ligands to cathepsin B. *J. Comput.-Aided Mol. Des.* **2011**, *25*, 729-742.

FOR TABLE OF CONTENTS ONLY

TEXT FOR GRAPHICAL ABSTRACT

The structure of twenty-five X-ray metallo*ligand*-protein structures with multiple vacant sites was successfully predicted by docking calculations, both in terms of binding site and metal coordination mode. The method, applied to the interaction between several potential metal drugs and proteins, allows to confirm the instrumental information or find additional hypotheses, and is generalizable to other metallodrugs and proteins.

GRAPHICAL ABSTRACT